Zygote

cambridge.org/zyg

Intranuclear characteristics of pig oocytes stained with brilliant cresyl blue and nucleologenesis of resulting embryos

Matej Murin[1], Frantisek Strejcek[4], Alexandra Bartkova[4], Martin Morovic[4], Michal Benc[2,4], Radek Prochazka[1], Andrea Lucas-Hahn[3], Lazo Pendovski[5] and Jozef Laurincik[1,4]

[1]Czech Academy of Sciences, Institute of Animal Physiology and Genetics, Rumburska 89, 277 21 Libechov, Czech Republic; [2]Institute of Animal Science, Pratelstvi 815, 10400 Prague Uhrineves, Czech Republic; [3]Friedrich Loeffler Institute, Institute of Farm Animal Genetics, Holtystrasse 10, D-31535 Neustadt, Germany; [4]Constantine the Philosopher University in Nitra, Faculty of Natural Sciences, Nabrezie mladeze 91, 94974 Nitra, Slovak Republic and [5]Ss. Cyril and Methodius University in Skopje, Republic of Macedonia.

Research Article

Cite this article: Murin M *et al.* (2019) Intranuclear characteristics of pig oocytes stained with brilliant cresyl blue and nucleologenesis of resulting embryos. *Zygote* **27**: 232–240. doi: 10.1017/S0967199419000352

Received: 22 February 2019
Revised: 6 May 2019
Accepted: 20 May 2019
First published online: 9 August 2019

Keywords:
Brilliant cresyl blue; Intranuclear characteristics; Nucleoli; Nucleologenesis of embryos; Pig.

Address for correspondence:
Matej Murin. Institute of Animal Physiology and Genetics CAS, v. v. i., Rumburska 89, 277 21 Libechov, Czech Republic. Tel: +420 315 639 544. E-mail: Murin@iapg.cas.cz

Summary

Brilliant cresyl blue (BCB) vital labelling is a powerful method for analyzing the quality of porcine cumulus–oocyte complexes. Our aim was to investigate the correlation between the selection of porcine oocytes using BCB labelling and selected intranuclear characteristics of porcine oocytes and parthenotes. Moreover, BCB labelling was correlated with the diameter of the oocyte and the developmental potential of the parthenotes. The following methods were used: BCB labelling, measurement of the diameter of the oocyte, parthenogenetic activation, immunocytochemistry, transmission electron microscopy, enucleation and relative protein concentration (RPC) analysis. We determined that the diameter of the oocytes in the BCB-positive (BCB+) group was significantly larger than in the BCB-negative (BCB−) group. Immediately after oocyte selection according to BCB labelling, we found significant difference in chromatin configuration between the analyzed groups. BCB+ oocytes were significantly better at maturation than BCB− oocytes. BCB+ embryos were significantly more competent at cleaving and in their ability to reach the blastocyst stage than BCB− embryos. Ultrastructural analyses showed that the formation of active nucleoli in the BCB+ group started at the 8-cell stage. Conversely, most BCB− embryos at the 8-cell and 16-cell stages were fragmented. No statistically significant difference in RPC in nucleolus precursor bodies (NPBs) between BCB+ and BCB− oocytes was found. We can conclude that BCB labelling could be suitable for assessing the quality of porcine oocytes. Moreover, the evaluation of RPC indicates that the quantitative content of proteins in NPB is already established in growing oocytes.

Introduction

Porcine oocytes are usually retrieved from the ovaries of slaughtered gilts, mixing oocytes of different quality obtained at different stages of the oestrous cycle (Ishizaki *et al.*, 2009). Strict criteria for evaluating oocyte quality before their submission for *in vitro* culture may increase the number of the oocytes suitable for *in vitro* embryo production. At present, the most frequent criterion for the selection of oocytes is their morphology, which mainly includes evaluating ooplasm granulation and the number of layers of cumulus cells. Recently, a series of biochemical methods based on biochemical markers has been developed to increase the rate of high quality oocytes retrieval from ovaries.

One of these methods is brilliant cresyl blue (BCB) vital labelling, which is based on the evaluation of glucose-6-phosphate dehydrogenase (G6PDH) activity as the marker of cytoplasmic maturation (Ishizaki *et al.*, 2009). This enzyme is synthesized in BCB-negative (BCB−) oocytes, which are still in the growing phase. BCB− oocytes enzymatically break down BCB and remain colourless. In oocytes that have finished their growth (BCB-positive oocytes, BCB+) this enzyme is inactivated and oocytes stain blue. The quality of BCB+ oocytes is higher than the quality of BCB− oocytes (Kempisty *et al.*, 2011; Antosik *et al.*, 2014). This test has been used in oocytes of different species including pigs, mice, goats, cattle and buffaloes (Opiela and Kątska-Książkiewicz, 2013). Conversely, a negative influence of double BCB staining on fertilization *in vitro*, cleavage and development to the blastocyst stage has been documented in pigs (Wongsrikeao *et al.*, 2006; Pawlak *et al.*, 2011). However, it is important to state that previously published data showed that single BCB staining is a highly effective method for the evaluation of oocyte quality, as they are still viable after BCB labelling (Kempisty *et al.*, 2011; Antosik *et al.*, 2014).

Evaluations of the germinal vesicle chromatin configuration in porcine oocytes and of the ultrastructure of nucleoli and immunolabelling of their key nucleolar proteins in *in vivo*-developed, *in vitro*-produced embryos and parthenotes have already been published (Bjerregaard *et al*., 2004; Sun *et al*., 2004; Deshmukh *et al*., 2012). However, in all these studies oocytes were not selected by BCB vital labelling before *in vitro* culture (Roca *et al*., 1998; Pujol *et al*., 2004). Therefore, the aim of our study was to investigate the correlation between the selection of porcine oocytes using BCB vital labelling and oocyte chromatin development during *in vitro* maturation (IVM), the ability to reach the metaphase II (MII) stage and the diameter of the oocytes, respectively. Moreover, BCB vital labelling was correlated with the developmental potential of the parthenotes, nucleologenesis, and the intranucleolar localization of upstream binding factor (UBF) and fibrillarin as markers of major embryonic genome activation. UBF is an indirect marker of transcriptional activities in nucleoli and fibrillarin is an indirect marker of post-transcriptional activities in nucleoli. We also analyzed the relative protein concentration (RPC) in the nucleolus precursor bodies (NPBs) of oocytes, because nucleoli and their content are important for embryonic development. As after BCB vital labelling cumulus–oocyte complexes (COCs) are still able to develop, this test presents an efficient way to analyze the quality of porcine COCs.

Materials and Methods

All chemicals were purchased from AppliChem (Darmstadt, Germany) unless otherwise stated. All plastic materials were purchased from Nunc (Roskilde, Denmark) unless otherwise stated.

Recovery of cumulus–oocytes complexes

Porcine ovaries were collected from prepubertal gilts at a local slaughterhouse. They were transported to the laboratory in a flask within 2 h of slaughter. Ovaries were washed three times with modified phosphate-buffered saline (mPBS) (0.4% (wt/vol) bovine serum albumin (BSA; Merck; Darmstadt, Germany), 0.34 mM glucose, 5.5 mM pyruvate, 50 IU/ml penicillin and 50 µg/ml streptomycin). COCs were aspirated from follicles from 3 to 6 mm in diameter using a 20-gauge needle attached to a 5-ml syringe (Sun *et al*., 2004). COCs were morphologically evaluated under a stereomicroscope (Nikon SMZ800N, Tokyo, Japan, × 45 magnification). Only those with an evenly granulated cytoplasm and at least three layers of cumulus cells were used for the experiments.

BCB vital labelling and measurement of diameter of oocytes

Before BCB vital labelling, COCs were washed three times in mPBS. They were then treated with 13 µM BCB in mPBS at 38.5°C in a humidified air atmosphere for 90 min. After this treatment, COCs were washed three times in mPBS. Finally, they were classified as BCB+ (blue cytoplasm) or BCB− (colourless cytoplasm) (Coy *et al*., 2005; Spikings *et al*., 2007).

For measuring diameter, COCs were washed three times in mPBS and were denuded by pipetting in PBS + 0.1% PVA with 0.1% hyaluronidase (Sigma-Aldrich, Munich, Germany). We measured two perpendicular diameters using a confocal laser scanning microscope (Zeiss LSM 710, Oberkochen, Germany, Zen blue software, ×20 magnification). The final diameter was determined as the mean value of these two perpendicular diameters (Pujol *et al*., 2004).

In vitro *maturation of oocytes and chromatin configuration*

After BCB vital labelling (Coy *et al*., 2005), COCs were washed three times in DMEM IVM medium. After that, COCs were transferred into DMEM medium in a 4-well dish and cultivated for 0, 4, 8, 12, 14, 16, 18, 20, 22, 24 or 40 h at 38.5°C in a 5% CO_2 in air atmosphere. The oocytes were transferred to DMEM IVM medium at 0 h.

After 0, 4, 8, 12, 14, 16, 18, 20, 22 or 24 h of cultivation in DMEM IVM medium, COCs were washed three times in mPBS and denuded as described above. To detect the germinal vesicle (GV) and later stages of chromatin configuration, oocytes were stained by incubation for 10 min in mPBS with 10 µg/ml Hoechst 33342 at 38.5°C in air. Oocytes were subsequently transferred in groups onto glass slides and squashed with coverslips, and then classified with a confocal laser scanning microscope (Zeiss LSM 710, Oberkochen, Germany, Zen blue software, ×40 magnification) into seven categories:

1. GV0 – with intact nucleolus and chromatin throughout the whole nuclear area.
2. GV1 – with intact nucleolus and chromatin in the form of a ring or horseshoe around the nucleolus.
3. GV2 – with the same characteristics as GV1 except for clumps of chromatin near the nuclear membrane.
4. GV3 – with intact nucleolus and chromatin in the form of a ring or horseshoe around the nucleolus, chromatin around the nuclear membrane and also condensed into strands and clumps dispersed throughout the whole nucleoplasm.
5. GV4 – without nucleolus, and chromatin condensed into clumps and strands throughout the whole nucleus.
6. Germinal vesicle breakdown (GVBD) – without nuclear membrane and chromosomes organized into an M plate.
7. Degenerated – without any signal (Sun *et al*., 2004; Fig. 1).

For detecting the first polar body, COCs were cultivated for 40 h in DMEM IVM medium at 38.5°C in a 5% CO_2 in air atmosphere. They were then washed three times in mPBS and denuded as described above. Oocytes were labelled by incubation for 15 min in mPBS containing 12 µg/ml Hoechst 33342 at 38.5°C in air. Finally, samples were prepared and evaluated as described above. Only oocytes with chromosomes organized into a M plate and with the first polar body were classified as MII oocytes (Fig. 1).

Parthenogenetic activation of oocytes and embryos cultivation

After 40 h IVM, cumulus cells from some COCs were removed as described above. Next, oocytes were cultured in TL-HEPES for 7 h at 38.5°C in a 5% CO_2 in air atmosphere and washed in sorbitol medium (250 mM sorbitol, 0.1 mM Ca-acetate, 0.5 mM Mg-acetate and 0.1% BSA(V), pH 7.2). Oocytes were then transferred to a chamber of a CF-150/B Electro-Cell Manipulator (BLS, Budapest, Hungary) with sorbitol medium. Oocytes were activated using a direct current pulse of 1.5 kV/cm lasting 100 µs. Oocytes were washed in TL-HEPES and chemically activated in porcine zygote medium-3 (PZM-3) (Yoshioka *et al*., 2002) containing a kinase inhibitor, 6-dimethylaminopurine (6-DMAP, 4 mM), for 3 h at 38.5°C in a 5% CO_2 in air atmosphere. Finally, oocytes were washed three times in PZM-3 and cultivated in PZM-3 under silicon oil (Silicone DC 200 fluid: 100 cst; Serva Electrophoresis GmbH, Germany, Heidelberg) for 24 h or 168 h. The presumed zygotes were transferred to PZM-3 medium without 6-DMAP at

https://doi.org/10.1017/S0967199419000352 Published online by Cambridge University Press

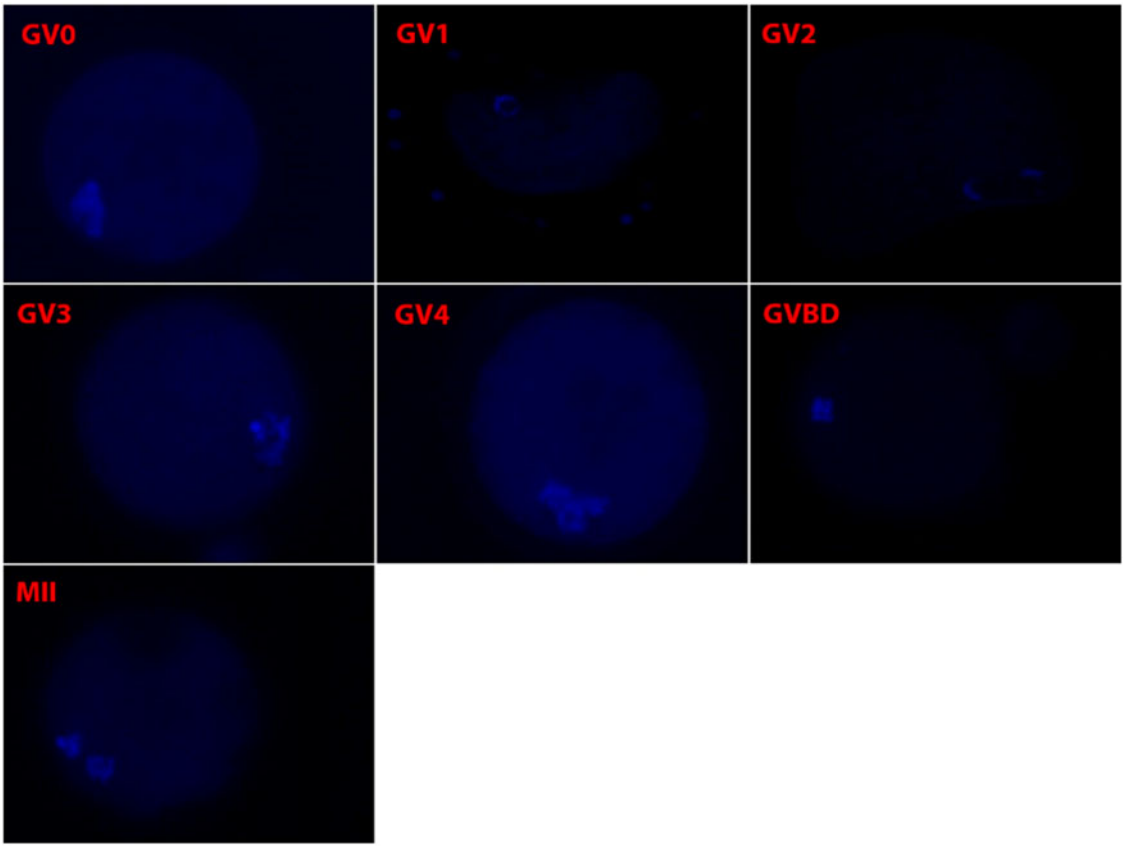

Figure 1. Development of chromatin configuration in porcine oocytes stained with Hoechst 33342 (×400 magnification).

0 h. After 24 h, embryo cleavage was evaluated and, after 168 h, the ability of embryos to reach the blastocyst stage was analyzed (Nikon SMZ800N, Tokyo, Japan, ×45 magnification). The number of cells in blastocysts was analyzed by cytochemical staining with propidium iodide (5 μg/ml) (Sigma-Aldrich, Munich, Germany) (described in the subsequent section).

Processing for light microscopy and transmission electron microscopy

BCB+ and BCB− 4-cell, 8-cell and 16-cell stage embryos were fixed in 3% glutaraldehyde in 0.1 M Na-phosphate buffer (pH 7.2). They were then washed in buffer, post-fixed in 1% OsO_4 in 0.1 M Na-phosphate buffer, embedded in Epon, and serially sectioned into semi-thin sections (2 μm). Every second section was stained with basic toluidine blue and evaluated by bright-field light microscopy. Selected semi-thin sections were re-embedded according to Hyttel and Madsen (1987) and processed for ultra-thin sectioning (70 nm). The ultra-thin sections were contrasted with uranyl acetate and lead citrate and examined in a Philips CM100 transmission electron microscope (Philips, Amsterdam, The Netherlands) (Hyttel and Madsen, 1987).

Immunocytochemistry and confocal laser scanning microscopy

The following primary antibodies against key nucleolar proteins were used: mouse anti-UBF (Abcam; Cambridge, UK) (1:50) and human anti-fibrillarin (1:500). For indirect immunofluorescence, 2-cell, 4-cell, 8-cell, 16-cell stage embryos and blastocysts were liberated from the zona pellucida by 0.5% pronase treatment and fixed in a mixture of 4% paraformaldehyde and 0.1% Triton X-100 for 3 h at 4°C. The specimens were then permeabilized in 0.5% Triton X-100 in PBS for 1 h at room temperature and blocked for 30 min in 2% BSA+0.5% Triton X-100 in PBS at room temperature. Thereafter, they were incubated with the primary antibody diluted in PBS for 1 h at room temperature. Excess primary antibody was removed by washing the specimens twice in 2% BSA+0.5% Triton X-100 in PBS for 30 min at room temperature. Next, specimens were incubated with the secondary antibody diluted in PBS: Alexa Fluor 488 goat anti-mouse (Thermo Fisher Scientific, Massachusetts, USA) (1:100, for mouse anti-UBF) or Alexa Fluor 488 goat anti-human (Thermo Fisher Scientific, Massachusetts, USA) (1:100, for human anti-fibrillarin) for 1 h at room temperature. Excess secondary antibody was removed by washing specimens twice in 2% BSA + 0.5% Triton X-100 in PBS for 30 min at room temperature. Finally, the specimens were mounted on glass slides using fluorescence mounting medium (Thermo Fisher Scientific, Massachusetts, USA) with propidium iodide (5 μg/ml) (Sigma-Aldrich, Munich, Germany) and examined using a Zeiss LSM 710 confocal laser scanning microscope (Zeiss, Oberkochen, Germany). Control immunostaining of non-specific labelling by the secondary antibodies was performed by omitting the primary antibodies and no immunocytochemical labelling was detected.

Enucleolation of oocytes

GV oocytes were enucleolated as described previously (Kyogoku *et al.*, 2012). Oocytes were transferred to PBS + 0.1%

https://doi.org/10.1017/S0967199419000352 Published online by Cambridge University Press

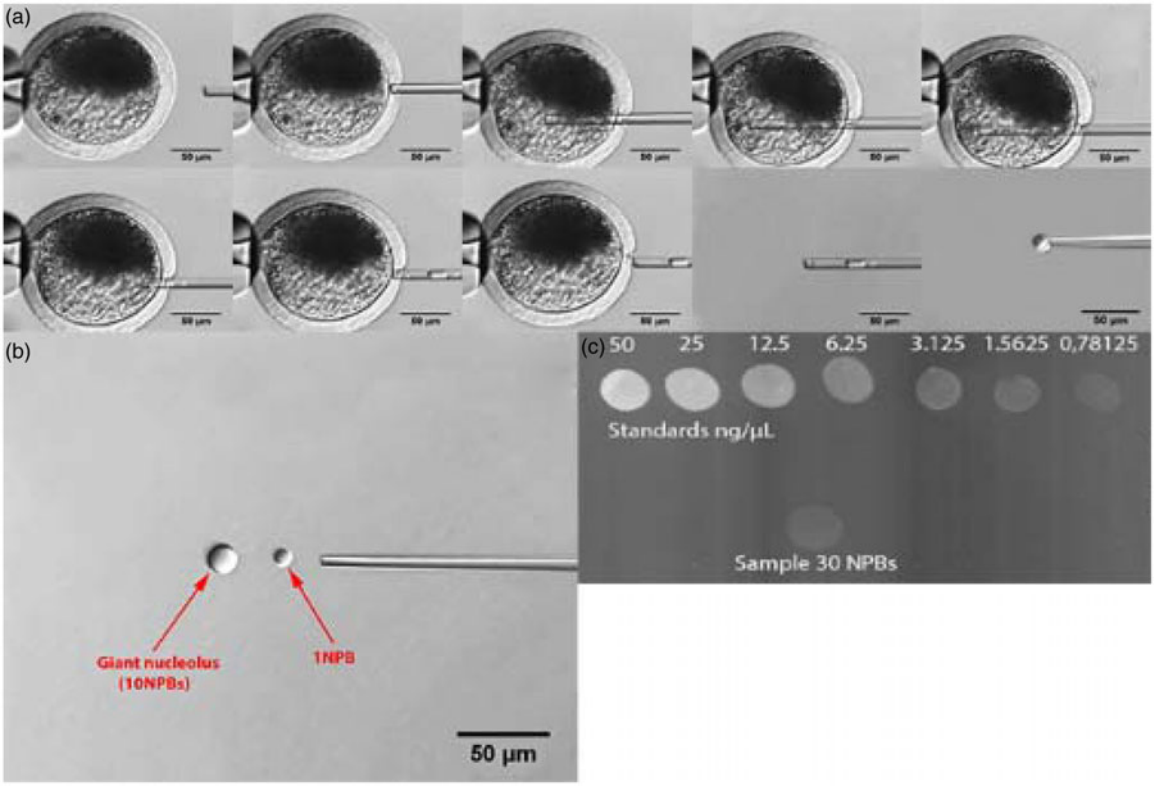

Figure 2. Enucleolation of porcine oocyte. (*A*) Process of enucleation. Scale bar: 50.0 µm. (*B*) The comparison of 1 NPB and 10 NPBs (giant nucleolus). NPB, nucleolus precursor body. Scale bar: 50.0 µm. (*C*) Relative protein concentration in NPBs of porcine oocytes. First row, standards in ng/µl; second row, sample.

PVA + 12.5 µg/ml cytochalasin B + 0.01 µg/ml demecolcine for 10 min. After that, oocytes were centrifuged at 6000 *g* for 10 min to move the ooplasm to one side of the oocytes. Oocytes were enucleolated in a micromanipulation chamber (IVF ICSI dish, 150265) on a warmed stage (38.5°C) of an inverted microscope (Zeiss LSM 710, Oberkochen, Germany) equipped with a micromanipulator (Eppendorf Transferman 4r, Hamburg, Germany). Each oocyte was held with a holding pipette (inner diameter 200 µm, angle 15°) at the 9 o'clock position. Then the oocyte was rotated until the nucleolus was at the 3 o'clock position. The zona pellucida was punctured at the 3 o'clock position using an injection pipette (inner diameter 10 µm, angle 15°) and piezo pulses. Piezo pulses were applied using a micromanipulator (Eppendorf Transferman 4r, Hamburg, Germany) equipped with a piezo drive (Eppendorf PiezoXpert, Hamburg, Germany). After penetration of zona pellucida, the injection pipette was positioned against the membrane of the GV. After that, gentle suction was used to draw the NPB into the pipette. The injection pipette was then withdrawn from the ooplasm. When the pipette was outside the cell membrane, further suction was applied. The NPB then penetrated the membrane of the GV and the entire nuclear content was left in the GV. Isolated NPBs were surrounded by plasma membrane (nucleoloplast) (Fig. 2A). Collected NPBs were fused together as described previously (Fulka *et al.*, 2012). Briefly, the nucleoloplast was broken using several high-frequency piezo pulses. Then the NPB was released from the pipette. Another NPB prepared in the same way was pushed against the first NPB, and the two merged as soon as they came into contact with each other. This step was repeated until the desired numbers of NPBs were merged. The result of this process was a giant nucleolus (Fig. 2B). Collected giant nucleoli were stored in PBS + 0.1% PVA in Protein LoBind tubes (Eppendorf 0030108094, Hamburg, Germany) at −80°C until they were used for RPC analysis.

Relative protein concentration in NPBs

Relative protein concentration was determined using colloidal gold staining. First, an Immun-Blot PVDF membrane (Bio-Rad 1620177) was immersed into methanol and then into Towbin's solution (0.025 M Tris, 0.192 M glycine, 20% methanol). After that, samples and standards were applied to the membrane (5 µl each). One sample consisted of 30 NPBs from GV oocytes. Various concentrations of BSA in PBS (50; 25; 12.5; 6.25; 3.125; 1.5625 and 0.78125 ng/µl) were used as standards. These were prepared from a BSA stock solution (5 mg/ml BSA in PBS). Next, the membrane was allowed to dry. The membrane was immersed into 50 ml of TTBS (Bio-Rad 1706435) + 0.6% Tween-20 on a shaker for 20 min. This step was repeated two more times. Then the membrane was washed three times in 50 ml of deionized water on a shaker for 2 min each. After that, the membrane was left in 20 ml of colloidal gold (Bio-Rad 170–6527) on a shaker for 18 h. After this period of time, the membrane was washed five times in 50 ml of deionized water on a shaker for 1 min each. The membrane was then allowed to dry and scanned using a laboratory scanner. The picture was inverted and analyzed using ImageJ software (Fig. 2C). The result of this analysis was the RPC.

Statistical analysis

At least three replicates were performed for each treatment. Our data were expressed as means ± standard error of the mean

https://doi.org/10.1017/S0967199419000352 Published online by Cambridge University Press

Table 1. Chromatin configuration at time 0 h (oocytes without cultivation) of porcine oocytes treated with BCB. Four replicates of this experiment were performed

Experimental group	GV0	GV1	GV2	GV3	GV4	GVBD	Degenerated
BCB+	21.30 ± 8.01%^{a}	29.62 ± 7.59%	8.67 ± 5.68%	8.98 ± 4.50%	27.44 ± 12.32%	0.00 ± 0.00%	4.00 ± 6.69%
BCB−	10.11 ± 6.50%^{b}	23.60 ± 6.16%	10.24 ± 7.51%	3.63 ± 4.04%	45.44 ± 10.18%	0.00 ± 0.00%	6.97 ± 6.25%

Within a column, values with different small letters (*a*, *b*) are significantly different at $P < 0.05$.

Table 2. Maturation ability of porcine oocytes treated with BCB *in vitro* and developmental potential of embryos after parthenogenetic activation. Five replicates of this experiment were performed. In brackets, number of oocytes or embryos are stated

Experimental group	% of metaphase II oocytes	% of embryos cleaved ± SEM	% of blastocysts ± SEM
BCB+	49.52 ± 3.36% (290)^{A}	58.87 ± 5.82 (166)^{A}	45.10 ± 6.58 (110)^{a}
BCB−	13.68 ± 5.31% (29)^{B}	15.20 ± 5.69 (8)^{B}	12.23 ± 7.02 (7)^{b}

Within a column, values with different capital letters (A, B) are significantly different at $P < 0.001$, and values with different small letters (*a*, *b*) are significantly different at $P < 0.05$. SEM, standard error of the mean.

(SEM). Oocyte diameters, meiotic competence, the development of embryos and the number of cells in blastocysts were analyzed by one-way analysis of variance (ANOVA) with Tukey's post-hoc test (SigmaPlot 12.0, London, UK). RPC experiments were analyzed using Kruskal–Wallis one-way ANOVA on ranks (SigmaPlot 12.0, London, UK). Chromatin configuration was analyzed by profile analysis with Tukey's post-hoc test in R (R, The R foundation for statistical computing). Differences between means of G6PDH activity of BCB+ and BCB− groups were tested using a *t*-test (SigmaPlot 12.0, London, UK). Probability values <0.05 were considered to be statistically significant.

Results

BCB vital labelling and measurement of diameter of oocytes

Altogether 468 COCs were used to analyze the ratio of BCB+ and BCB− COCs. Six replicates of this experiment were performed. The mean proportion of COCs classified as BCB− (28.11 ± 14.19%) was lower than that classified as BCB+ (71.89 ± 14.19%) ($P < 0.001$).

In total, 49 BCB+ and 29 BCB− oocytes were used to determine their diameters. Three replicates of this experiment were performed. Difference was identified in the diameter of oocytes between the BCB− group (117.99 ± 1.02 μm) and the BCB+ group (122.21 ± 0.92 μm) ($P < 0.01$).

Chromatin configuration

Altogether 1009 BCB+ and 437 BCB− oocytes were used to analyze their chromatin configuration. In accordance with our analysis of GV chromatin configuration, oocytes were divided into seven categories (GV0, GV1, GV2, GV3, GV4, GVBD and degenerated) as described above (see Materials and Methods). Difference was detected at time 0 h (oocytes without cultivation) in the GV0 category between the BCB− group and the BCB+ group ($P < 0.05$) (Table 1). No other statistically significant differences were found. GVBD started in BCB+ and BCB− groups at 12 h after the beginning of oocyte culture.

In total, 567 BCB+ and 179 BCB− oocytes were used to determine their maturation ability. BCB+ porcine oocytes were more competent to reach MII than BCB− porcine oocytes ($P < 0.001$) after 40 h of IVM (Table 2).

Cleavage of parthenogenetic embryos

Altogether 595 BCB+ and 204 BCB− COCs were used to determine their embryonic development after parthenogenetic activation. Difference in the ability of the embryos to reach the 2-cell stage was found between the BCB− group and the BCB+ group ($P < 0.001$). Difference was detected in the ability of the embryos to reach the blastocyst stage between the BCB− group and the BCB+ group ($P < 0.05$) (Table 2). Most BCB− embryos were able to reach only the 2-cell or 4-cell stage. The proportion of these two stages was the same. The difference in the number of cells in blastocysts between the BCB− group ($n = 32.43 \pm 12.64$) and the BCB+ group ($n = 44.50 \pm 16.22$) was not statistically significant.

Nucleologenesis in early embryos

In total, 12 replicates of this experiment were performed. All nuclei in five BCB+ 4-cell stage embryos exhibited one or two NPBs, consisting of densely packed fibrils within each nucleus (Fig. 3A). In BCB− embryos, a similar picture was seen in two embryos. The other two embryos were fragmented and degenerated.

In six BCB+ 8-cell stage embryos, all nuclei exhibited both compact and vacuolated NPBs, indicating rDNA genome activation and beginning the transformation of NPBs into a functional, transcriptionally active nucleolus (Fig. 3B). A similar picture in BCB− embryos was only observed in one embryo. The other five BCB− embryos were fragmented and degenerated.

In BCB+ 16-cell stage embryos, all nuclei in three out of four embryos exhibited both compact and vacuolated NPBs, as observed in earlier embryonic stages, and also transcriptionally active reticulated nucleoli exhibiting fibrillar centres (FC), dense fibrillary components (DFC), and granular components (GC). One embryo was fragmented and degenerated (Fig. 3C). In the BCB− group, seven out of eight sectioned embryos were fragmented and degenerated. The nuclei of one BCB− embryo contained transcriptionally active reticulated nucleoli exhibiting FC, DFC and GC.

Immunocytochemistry and confocal laser scanning microscopy

Because of the low developmental potential of BCB− embryos, they were not immunocytochemically analyzed except for blastocysts. The numbers of positively, positively/negatively (only some blastomeres were positively stained) and negatively stained embryos, apart from 2-cell stage embryos, are shown in Tables 3 and 4.

https://doi.org/10.1017/S0967199419000352 Published online by Cambridge University Press

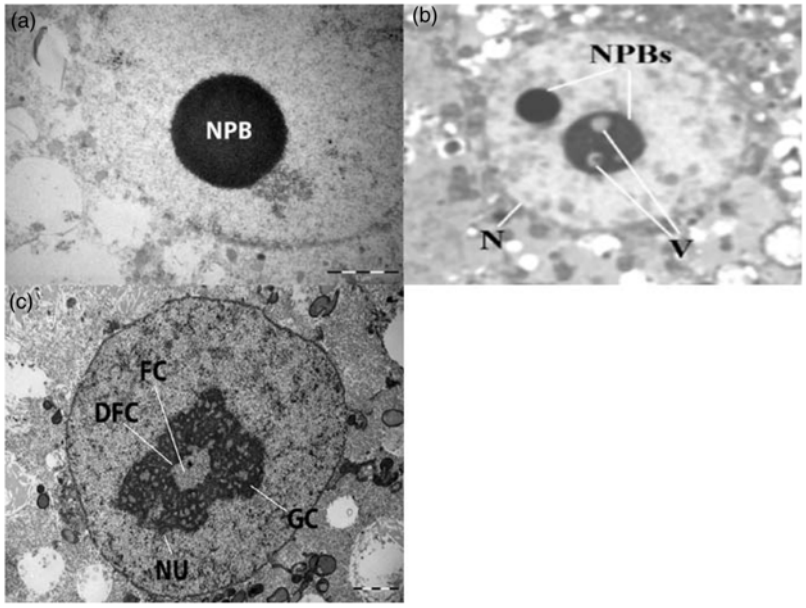

Figure 3. Nucleologenesis in porcine embryos. (*A*) Nucleolus precursor body (NPB) of porcine 4-cell BCB+ embryo. Scale bar: 1.0 μm. (*B*) Nucleus (N) of porcine 8-cell BCB+ embryo. NPBs, nucleolus precursor bodies; V, vacuole (×1000 magnification). (*C*) Active fibrillo-granular nucleolus (NU) of 16-cell BCB+ porcine embryo. DFC, dense fibrillary components; FC, fibrillar centres; GC, granular components. Scale bar: 2.0 μm.

Table 3. Immunocytochemical detection of upstream binding factor

	Upstream binding factor (no. of embryos analyzed)		
BCB+	+	±	–
4-cell	0	0	6
8-cell	6	3	0
16-cell	8	0	0
BCB–	+	±	–
Blastocysts	2	0	0

+, all blastomeres were positively stained. ±, only some blastomeres were positively stained, –, no blastomeres were positively stained. Three replicates of this experiment were performed.

Table 4. Immunocytochemical detection of fibrillarin

	Fibrillarin (no. of embryos analyzed)		
BCB+	+	±	–
4-cell	0	0	7
8-cell	4	4	0
16-cell	7	0	0
BCB–	+	±	–
Blastocysts	2	0	0

+, all blastomeres were positively stained. ±, only some blastomeres were positively stained, –, no blastomeres were positively stained. Three replicates of this experiment were performed.

Because of no signal in 2-cell and 4-cell stage BCB+ embryos, 1-cell stage BCB+ embryos were not analyzed. In 8-cell stage BCB+ embryos, labelling of UBF (Fig. 4A and Table 3) and fibrillarin (Fig. 4B and Table 4) was detected. UBF was localized to small foci in the FC of fibrillo-granular nucleoli. Fibrillarin was localized to circles in the DFC of fibrillo-granular nucleoli. In 16-cell stage BCB+ embryos, the same immunocytochemical characteristics were observed as at the 8-cell stage, but in all nuclei. BCB– blastocysts were analyzed immunocytochemically and the same immunocytochemical features were observed as depicted for the 16-cell stage of BCB+ embryos (Fig. 4C, D).

Relative protein concentration in NPBs

In total, 90 NPBs from both experimental groups (BCB+ and BCB–) obtained by enucleation were used to analyze the RPC in NPBs of porcine oocytes. Three replicates of this experiment were performed. No statistically significant difference between the BCB+ (0.93 ± 0.01 ng/NPB) and BCB– (0.91 ± 0.01 ng/NPB) group was found.

Discussion

The *in vitro* cultivation of porcine oocytes and embryos might be improved by using a combination of the standard analysis of morphology of the oocytes supplemented with various biochemical tests. In this study, a combination of morphological analysis and BCB vital labelling, which was based on the evaluation of enzyme G6PDH activity, were used. To determine the developmental potential of the oocytes, G6PDH activity was correlated with the diameter, chromatin configuration and meiotic competence of oocytes and the RPC in NPBs, as well as the cleavage rate and major embryonic genome activation at the ultrastructural and immunocytochemical level.

As for oocyte diameter in pigs, our findings are in agreement with the study of Roca *et al.* (1998). In pigs they found that BCB+ oocytes were significantly larger than BCB– oocytes. Diameter is very important feature of porcine oocytes. Size of porcine oocytes is increasing with increasing diameter of follicles (Lucas *et al.*, 2002). Porcine oocytes acquired the ability to complete meiotic maturation in antral follicles of about 2 mm in diameter. At this point, there was a significant decrease in the nucleolar transcriptional activity of the oocytes, which is important for storage of some information indispensable to the initiation and completion of the first meiotic division. Synthesis of ribosomal RNAs is connected to the synthesis of messenger RNAs (mRNAs). Absence or insufficiency of mRNAs coding for a cytoplasmic factors could interfere with the ability of oocytes to resume meiotic maturation because of lower quality cytoplasmic content (Motlik *et al.*, 1984).

https://doi.org/10.1017/S0967199419000352 Published online by Cambridge University Press

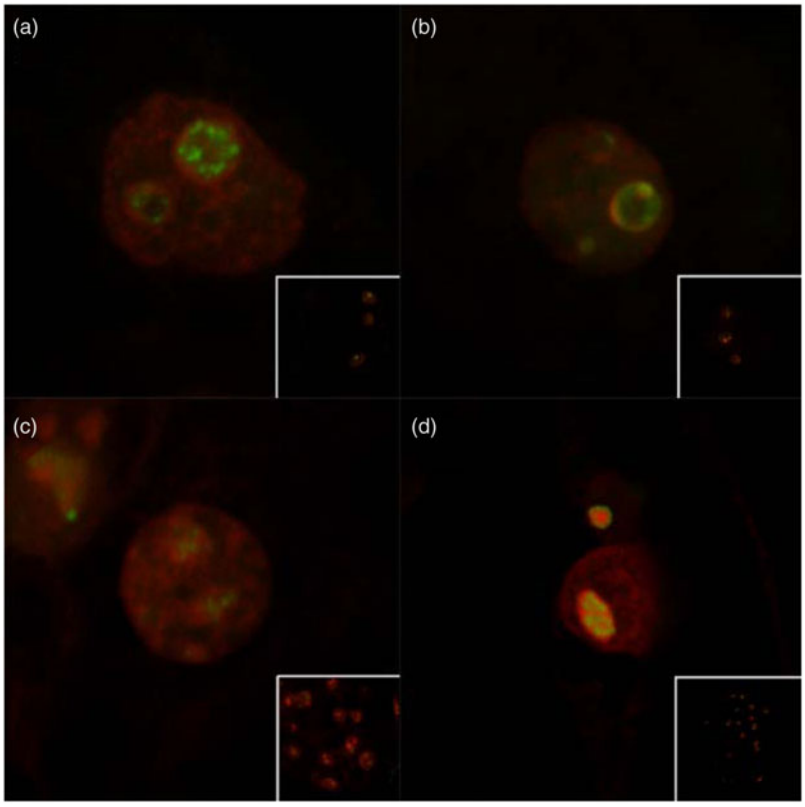

Figure 4. Detection of upstream binding factor (UBF) and fibrillarin in porcine embryos. (*A*) Detection of UBF in 8-cell BCB+ embryos: green, UBF; red, propidium iodide (detection of DNA) (×630 magnification). Main panel: detail on the nucleus. Insert: whole embryo. (*B*) Detection of fibrillarin in 8-cell BCB+ embryo: green, fibrillarin; red, propidium iodide (detection of DNA) (×630 magnification). Main panel: detail on the nucleus. Insert: whole embryo. (*C*) Detection of UBF in BCB− blastocyst: green, UBF; red, propidium iodide (detection of DNA) (×400 magnification). Main panel: detail on the nucleus. Insert: whole embryo. (*D*) Detection of fibrillarin in BCB− blastocyst: green, fibrillarin; red, propidium iodide (detection of DNA) (×400 magnification). Main panel: detail on the nucleus. Insert: whole embryo.

Chromatin configuration has been analyzed previously in porcine oocytes by Sun *et al.* (2004), but not after BCB staining. Pan *et al.* (2018) published a newer classification of chromatin in porcine GV oocytes. In this classification, there were more categories of chromatin configuration, because they also analyzed premature condensation of chromatin (Pan *et al.*, 2018). We used the classification of Sun *et al.* (2004), because our analysis of chromatin configuration was already completed at the time of publication of the Pan *et al.* (2018) research paper. Sun *et al.* (2004) observed that GV0 oocytes disappeared from follicles with a diameter from 2 to 6 mm. In our study, only oocytes from follicles with a diameter from 3 to 6 mm were used. However, we detected the GV0 stage from 0 h to 24 h of IVM. The reason for this result could be the presence of atretic follicles in our study, as we did not differentiate healthy follicles from atretic ones, as did the other group. At time 0 h (oocytes without cultivation), the percentage of BCB+ oocytes at the GV0 stage was statistically significantly higher than in BCB− oocytes. The proportion of oocytes with the GV2 chromatin configuration during IVM was similar in our study to that of Sun *et al.* (2004). Possibly these oocytes were unable to continue maturation or their follicles started to develop towards atresia. Observations during the growth and maturation of the oocytes suggest that GV2, GV3 and GV4 stages of chromatin development could be more advanced toward ovulation. Another explanation could be that these changes were due to effects occurring before atresia. Therefore, our observations in GV3 and GVBD stage oocytes could represent those that are more advanced toward ovulation, but also those in which follicles are more advanced to atresia, depending upon the circumstances (Sun *et al.*, 2004; Egerszegi *et al.*, 2010).

When porcine BCB+ and BCB− oocytes were fertilized *in vitro*, there were no statistically significant differences in the ability of embryos to cleave (Wongsrikeao *et al.*, 2006) or to reach the blastocyst stage (Ishizaki *et al.*, 2009). Opiela *et al.* (2008) found that *in vitro*-matured and *in vitro*-fertilized (IVM/IVF) bovine BCB+ oocytes were significantly better in their ability to reach the 2-cell stage and blastocyst stage than BCB− oocytes. We observed that a significantly higher number of the embryos obtained from BCB+ oocytes were able to cleave and to reach the blastocyst stage than the embryos originating from BCB− oocytes. The difference between parthenogenetic activation and IVF could be the reason for the discrepancies between our data and those observed after IVF. Heleil *et al.* (2010) found that bovine BCB+ blastocysts obtained after IVM/IVF had a significantly higher total cell number than BCB− blastocysts. In this study we did not find any statistically significant difference in total cell number of blastocysts after parthenogenetic activation between BCB+ and BCB− group.

In parthenogenetically produced porcine 4-cell stage embryos, Deshmukh *et al.* (2012) observed two to four NPBs per cell without detecting fibrillo-granular nucleoli. However, in 8-cell/morula stage embryos, they detected fibrillo-granular nucleoli in all blastomeres. As the authors merged all the development stages from the 8-cell stage to the end of the morula stage their conclusion is not clear. The 8-cell stage is very important in pigs in the processes analyzed by the authors of the above paper. Therefore, it is important to analyze the 8-cell and 16-cell stage separately. In our study, we differentiated 8- and 16-cell stage embryos. At the 8-cell stage only NPBs were seen, however, at the 16-cell stage, both NPBs and fibrillo-granular nucleoli were detected. These observations are supported by our previous study (Hyttel *et al.*, 2000) on 16-cell stage porcine embryos, in which both NPBs and fully functional nucleoli composed of FC, DFC and GC were exhibited. The ultrastructural analysis of BCB− embryos showed that most of the 8-cell and 16-cell stage embryos were fragmented and degenerated, which is also documented by their lower developmental capacity to the blastocyst stage compared with BCB+ group embryos. This finding could be explained by insufficient major embryonic

https://doi.org/10.1017/S0967199419000352 Published online by Cambridge University Press

genome activation in the BCB− group embryos. This idea is supported by our previous experiments in porcine embryos produced by *in vitro* fertilization (Laurincik *et al*., 2004), in which the major embryonic genome activation started one or two developmental stages later than the major embryonic genome activation observed in porcine *in vivo*-developed embryos (Hyttel *et al*., 2000). Another reason for the worse developmental potential of BCB− embryos compared with BCB+ embryos could be lower mitochondrial DNA copy number in both unfertilized and fertilized BCB− oocytes compared with unfertilized BCB+ and fertilized BCB+ oocytes, respectively (Shourbagy *et al*., 2006).

In *in vivo*-developed porcine embryos, UBF and fibrillarin labelling of NPBs was not observed until the 8-cell stage (Hyttel *et al*., 2000). These data are in accordance with our results observed in BCB+ embryos. Moreover, these results were clearly in harmony with the ultrastructural observations of nucleologenesis in BCB+ embryos performed in this study. Based on our immunocytochemical and ultrastructural analysis, we can assume that in BCB+ embryos obtained after parthenogenetic activation, there were no transcriptional and post-transcriptional activities in nucleoli until the 8-cell stage. In this study a small proportion of BCB− blastocysts exhibited UBF and fibrillarin labelling in fully functional nucleoli, demonstrating sufficient major embryonic genome activation in a very small amount of BCB− embryos.

In this study we found that there was no statistically significant difference in the RPC of NPBs from BCB+ and BCB− porcine oocytes. These data indicated that the quantitative content of proteins in NPB is already established in growing oocytes. However, more analyses are required to fully understand the proteome of NPBs. Perhaps the difference could be in the quality of the NPB proteome from these groups of porcine oocytes. Therefore, the next step could be mass spectrometry analysis. Interestingly, Fulka *et al*. (2012) found that the RPC of NPBs from murine oocytes (1.6 ± 0.3 ng/NPB) was 1.7-fold higher than we observed in our experiments with NPBs aspirated from porcine oocytes.

In conclusion, we demonstrated that the activity of G6PDH in porcine oocytes detected using BCB vital labelling was associated with chromatin configuration, oocyte diameter, embryo cleavage and the development of active fibrillo-granular nucleoli in embryos after parthenogenetic activation. Conversely, we did not find any significant difference between the BCB+ and BCB− groups in the number of cells in blastocysts. Also, no statistically significant difference in the RPC of NPBs from these groups was found. We found that BCB vital labelling can help in the selection of oocytes with a larger diameter. Subsequently, these oocytes are more competent to reach the MII stage and, after parthenogenetic activation, they also have a better developmental potential. Therefore, it could be concluded that BCB vital labelling is a suitable method for assessing the quality of porcine oocytes.

Acknowledgements. We gratefully acknowledge the Microscopy Centre, Electron Microscopy Core Facility, IMG ASCR, Prague, Czech Republic, supported by the MEYS CR (LM2015062 Czech-BioImaging) for performing ultrathin sectioning of embryos.

Ethics statements. The authors assert that all procedures contributing to this work comply with the ethical standards of the relevant national and institutional guides on the care and use of laboratory animals.

Financial support. This work was supported by the Slovak Research and Development Agency (J.L., grant number APVV-14-0001); the Operational Programme Research, Development and Education (J.L., grant number CZ.02.1.01/0.0/0.0/15_003/0000460); the Danish Council for Independent Research/Natural Sciences (FNU) (J.L., grant number 8021-00048B); and the Ministry of Education, Science, Research and Sport of the Slovak Republic (J.L., grant numbers VEGA 1/0022/15, VEGA 1/0001/19), (F.S., grant number VEGA 1/0327/16).

Statement of interest. None.

References

Antosik P, Kempisty B, Piotrowska H, Bukowska D, Ciesiolka S, Jeseta M, Piescikowska I, Lange K, Maryniak H, Jaskowski JM, Brussow KP, Nowicki M and Zabel M (2014) Expression of integrin beta 2 (ITGB2) and zona pellucida glycoproteins (ZP3, ZP3α) in developmentally competent and incompetent porcine oocytes. *Med Weter* **70**, 417–21.

Bjerregaard B, Wrenzycki C, Strejcek F, Laurincik J, Holm P, Ochs RL, Rosenkranz C, Callesen H, Rath D, Niemann H and Maddox-Hyttel P (2004) Expression of nucleolar-related proteins in porcine preimplantation embryos produced *in vivo* and *in vitro*. *Biol Reprod* **70**, 867–76.

Coy P, Romar R, Ruiz S, Canovas S, Gadea J, Vasquez FG and Matas C (2005) Birth of piglets after transferring of *in vitro*-produced embryos pre-matured with R-roscovitine. *Reproduction* **129**, 747–55.

Deshmukh RS, Østrup O, Strejcek F, Vejlsted M, Lucas-Hahn A, Petersen B, Li J, Callesen H, Niemann H and Hyttel P (2012) Early aberrations in chromatin dynamics in embryos produced under *in vitro* conditions. *Cell Reprogram* **14**, 225–34.

Egerszegi I, Alm H, Ratky J, Heleil B, Brussow KP and Torner H (2010) Meiotic progression, mitochondrial features and fertilization characteristics of porcine oocytes with different G6PDH activities. *Reprod Fertil Dev* **22**, 830–8.

Fulka H JR, Martinkova S, Kyogoku H, Langerova A and Fulka JJR (2012) Production of giant mouse oocyte nucleoli and assessment of their protein content. *J Reprod Develop* **58**, 371–6.

Heleil B, Kuzmina T, Novikova N, Torner H and Alm H (2010) Effect of prolactin on developmental competence of bovine oocytes selected by brilliant cresyl blue staining. *J Reprod Infertil* **1**, 1–7.

Hyttel P and Madsen I (1987) Rapid method to prepare mammalian oocytes and embryos for transmission electron microscopy. *Acta Anat* **129**, 12–4.

Hyttel P, Laurincik J, Rosenkranz Ch, Rath D, Niemann H, Ochs RL and Schellander K (2000) Nucleolar proteins and ultrastructure in preimplantation porcine embryos developed *in vivo*. *Biol Reprod* **63**, 1848–56.

Ishizaki C, Watanabe H, Bhuiyan MMU and Fukui Y (2009) Developmental competence of porcine oocytes selected by brilliant cresyl blue and matured individually in a chemically defined culture medium. *Theriogenology* **72**, 72–80.

Kempisty B, Jackowska M, Piotrowska H, Antosik P, Wozna M, Bukowska D, Brussow KP and Jaskowski JM (2011) Zona pellucida glycoprotein 3 (pZP3) and integrin β2 (ITGB2) mRNA and protein expression in porcine oocytes after single and double exposure to brilliant cresyl blue test. *Theriogenology* **75**, 1525–35.

Kyogoku H, Ogushi S and Miyano T (2012) Nucleoli from two-cell embryos support the development of enucleolated germinal vesicle oocytes in the pig. *Biol Reprod* **87**, 1–6.

Laurincik J, Bjerregaard B, Strejcek F, Rath D, Niemann H, Rosenkranz C, Ochs RL and Maddox-Hyttel P (2004) Nucleolar ultrastructure and protein allocation in *in vitro* produced porcine embryos. *Mol Reprod Dev* **68**, 327–34.

Lucas X, Martinez EA, Roca J, Vazquez JM, Gil MA, Pastor LM and Alabart JL (2002) Relationship between antral follicle size, oocyte diameters and nuclear maturation of immature oocytes in pigs. *Theriogenology* **58**, 871–85.

Motlik J, Crozet N and Fulka J (1984) Meiotic competence *in vitro* of pig oocytes isolated from early antral follicles. *J Reprod Fertil* **72**, 323–8.

Opiela J and Kątska-Książkiewicz L (2013) The utility of Brilliant Cresyl Blue (BCB) staining of mammalian oocytes used for *in vitro* embryo production (IVP). *Reprod Biol* **13**, 177–83.

Opiela J, Kątska-Książkiewicz L, Lipinski D, Słomski R, Bzowska M and Rynska B (2008) Interactions among activity of glucose-6-phosphate

https://doi.org/10.1017/S0967199419000352 Published online by Cambridge University Press

dehydrogenase in immature oocytes, expression of apoptosis-related genes Bcl-2 and Bax, and developmental competence following IVP in cattle. *Theriogenology* **69**, 546–55.

Pan LZ, Zhu S, Zhang M, Sun MJ, Lin J, Chen F and Tan JH (2018) A new classification of the germinal vesicle (GV) chromatin configurations in pig oocytes. *Biol Reprod* **99**, 1149–58.

Pawlak P, Pers-Kamczyc E, Renska N, Kubickova S and Lechniak D (2011) Disturbances of nuclear maturation in BCB positive oocytes collected from peri-pubertal gilts. *Theriogenology* **75**, 832–40.

Pujol M, Lopez-Bejar M and Paramio MT (2004) Developmental competence of heifer oocytes selected using the brilliant cresyl blue (BCB) test. *Theriogenology* **61**, 735–44.

Roca J, Martinez E, Vazquez JM and Lucas X (1998) Selection of immature pig oocytes for homologous *in vitro* penetration assays with the brilliant cresyl blue test. *Reprod Fertil Dev* **10**, 479–85.

Shourbagy SHE, Spikings EC, Freitas M and John JCS (2006) Mitochondria directly influence fertilisation outcome in the pig. *Reproduction* **131**, 233–45.

Spikings EC, Alderson J and John JCS (2007) Regulated mitochondrial DNA replication during oocyte maturation is essential for successful porcine embryonic development. *Biol Reprod* **76**, 327–35.

Sun XS, Liu Y, Yue KZ, Ma SF and Tan JH (2004) Changes in germinal vesicle (GV) chromatin configurations during growth and maturation of porcine oocytes. *Mol Reprod Dev* **69**, 228–34.

Wongsrikeao P, Otoi T, Yamasaki H, Agung B, Taniguchi M, Naoi H, Shimizu R and Nagai T (2006) Effects of single and double exposure to brilliant cresyl blue on the selection of porcine oocytes for *in vitro* production of embryos. *Theriogenology* **66**, 366–72.

Yoshioka K, Suzuki C, Tanaka A, Anas IMK and Iwamura S (2002) Birth of piglets derived from porcine zygotes cultured in a chemically defined medium. *Biol Reprod* **66**, 112–9.

https://doi.org/10.1017/S0967199419000352 Published online by Cambridge University Press